

[Click to View Poster](#)

## **Fully Controlled Sampling Workflow for Multi-Scale X-Ray Imaging of Complex Reservoir Rock Samples to be Used for Digital Rock Physics\***

**Sven Roth<sup>1</sup>, Youli Hong<sup>2</sup>, Hrishikesh Bale<sup>2</sup>, Tianpeng Zhao<sup>1</sup>, Sreenivas Bhattiprolu<sup>2</sup>, Matthew Andrew<sup>2</sup>, Chai Weichao<sup>1</sup>, Jeff Gelb<sup>2</sup>, and Benjamin Hornberger<sup>2</sup>**

Search and Discovery Article #41840 (2016)

Posted July 25, 2016

\*Adapted from extended abstract prepared in relation to poster presentation and from the presentation itself given at GEO 2016, 12th Middle East Geosciences Conference & Exhibition, Manama, Bahrain, March 7-10, 2016

\*\*Datapages © 2016 Serial rights given by author. For all other rights contact author directly.

<sup>1</sup>iRock Technologies, Beijing, China ([s.roth@irocktech.com](mailto:s.roth@irocktech.com))

<sup>2</sup>Carl Zeiss X-ray Microscopy, Pleasanton, CA, United States

### **Abstract**

Digital rock physics is a technique to simulate petrophysical properties and fluid flow parameters on digitized rock samples and, as such, requires multi-scale imaging from the pore scale to the plug scale (or core scale). This is straightforward for homogeneous sandstones, which often need only one scale of imaging because the size range of the pore network carrying the flow is very narrow. More heterogeneous rocks such as complex carbonates and tight sands require a sophisticated subsampling strategy including physical drilling, laser ablation, and multi-scale X-ray scanning with resolution from several micrometers down to nanometer size.

The challenge with complex rock types is that the facies of interest to be imaged at high resolution may be distributed somewhere inside the rock sample and has to be physically extracted once the region of interest is spotted. The facies of interest for high-resolution imaging of carbonates is mostly the microcrystalline rock phase (micrite; microporosity), which is distributed in the rock in varying amounts. In the case of tight sands very often the clay phase is of major interest. Especially, if the clay volume in the rock is very low the extraction of the target volume has to be very precise in the range of hundreds of microns.

Here we present a novel workflow for fully controlled subsampling of carbonates and tight sand reservoir rock samples for multi-scale 3D X-ray imaging at resolution from the microns to the tens of nanometers. The workflow is illustrated on one of the most challenging rock types in terms of subsampling and multi-scale imaging: a tight sand sample where minor and unevenly spread clay content governs the entire flow in the sample.

## Introduction

In the recent years, digital rock physics (DRP) and pore network modeling have developed into a tool for reservoir rock characterization, which is progressively being accepted by the oil and gas industry (Kalam et al., 2010; Schembre-McCabe et al., 2012; Kalam, 2012; Blunt et al., 2013, Al-Ratrou et al., 2014).

Continuous improvement of individual 3D-imaging devices now allows imaging of rock samples from the core scale down to nanometer scale, revealing the complex pore structures of different rock facies - a pre-requisite to achieve accurate predictions of petrophysical properties and multiphase fluid flow properties from pore-space images. However, there is no imaging device that can capture a whole core or even a core plug and, at the same time, resolve the pore space at a sufficient resolution. Moreover, due to computational constraints it is not currently possible to combine large-scale rock features (centimeter to millimeter) with sub-micron information into one single 3D rock model. Therefore, petrophysical properties and multi-phase flow properties have to be simulated on smaller-scale subsample images and have to be incorporated within a unique predictive modelling framework to provide upscaled flow and transport.

Precise sub-sampling and imaging routines, as discussed herein, and the accuracy of upscaling techniques lead to significantly improved models, which are conducive to robust predictions at the field-scale and as such impact reservoir management and improved oil recovery. [Figure 1](#) indicates the position of such a multi-scale subsampling and imaging module in a generalized DRP workflow. Careful subsample selection and sample preparation is, thus, an extremely important part of a successful DRP work flow; especially if there are constraining parameters to be considered, such as the size of the field of view (FOV), required optimal X-ray transmission, sufficient contrast and a good signal to noise ratio. The prescriptive sample preparation workflow presented here, enables a user to start with the imaging of a large sample (1" or 1.5" core plug) on a micro-CT (MCT) machine and provides a means to target and isolate a specific 65  $\mu\text{m}$  diameter sub volume of interest from that large sample.

The workflow consists of alternating steps of sample preparation and imaging on a MCT machine at different resolutions until the final nanoCT imaging sample size is reached. Basic guidelines are suggested beginning with the selection of regions of interest followed by targeted sample preparation through physical drilling and with a laser micromachining system, and final 3D imaging on a nanoCT device at highest resolutions. The workflow detailed here may need case-by-case procedural modifications depending on sample starting size, geometry of specimen and imaging requirements.

## Material, Methods and Results

The rock sample is a tight sandstone composed of medium sand sized grains up to 500  $\mu\text{m}$  in diameter. The pore space is intensely cemented, which resulted in partly closure of the pore throats. The remaining larger pores (up to 250  $\mu\text{m}$  size) are entirely filled by clay minerals - mainly aggregates of kaolinite platelets, such that all flow has to pass through these clay volumes. Therefore, the clay and the pore space between the kaolinite aggregates governs the flow in this rock and have to be studied in detail in order to simulate petrophysical properties.

*General description of the workflow.* The workflow starts with a MCT scan of a 1-1.5” diameter core plug sample. Then a 4-5 mm diameter mini-plug is mechanically drilled out and imaged in a MCT with voxel size of 2.5 to 5 microns. Based on this 3D dataset, a region of interest (ROI) for higher resolution subsampling is identified, and a ~1 mm diameter pillar centered on the ROI is extracted using a laser machining system. After high resolution MCT imaging with about 1 micron voxel size, this pillar is further reduced in size to about 65 microns diameter using the same laser machining system, operated in a rotational lathe mode. This micro-pillar can then be imaged at ultra-high resolution in a nanoscale

*X-ray microscope (nanoCT) with 65 nm voxel size.* The 3D datasets acquired are used to simulate petrophysical and multi-phase fluid flow properties of the reservoir rock samples and for subsequent upscaling of these properties to core plug scale. Based on the specific heterogeneity and other characteristics of the reservoir, the workflow can be tailored to image at different sample size and resolution levels. [Figure 2](#) gives a schematic and graphical overview about the entire subsampling and imaging workflow. The detailed work steps are given in the subsequent sections.

*Instrumental set-up.* Physical subsampling by drilling was performed with a Proxxon Core drill (4-5 mm). However, a standard core drill with a broad range of drill-bit diameters can easily be purchased. Core drilling should be performed on dedicated core drilling equipment, a drill press or on a vertical milling machine with appropriate equipment to hold the sample securely while drilling. All MCT images were acquired with an Xradia 520 Versa XRM machine; the nanoCT images with an Xradia 810 Ultra XRM. The Oxford Lasers A-532-DW system was used for laser micromachining in “top-down” mode and in the horizontal “lathe-style” mode.

*Detailed Work Flow.* The following steps list the detailed procedure involved in a multi-scale imaging workflow applied to a tight sand sample, similar to the one shown in [Figure 2](#). Multi-scale 3-D imaging was performed, ranging from a resolution of several microns to a few tens of nanometers, covering a field of view (FOV) range from 4 mm to 65  $\mu\text{m}$ . The features of interest in this particular sample were porous clay structures, filling the pores between large cemented sand grains. These aggregates of kaolinite platelets typically range from tens of nanometers to a few microns. Although the overall clay volume in this sample is very sparse (< 5%), it is the porosity between the kaolinite aggregates that connects this very tight and cemented rock. Proper sampling and imaging of this clay phase is therefore crucial for simulation of flow in subsequent DRP analysis.

#### Step I - Full-field-of-view MCT imaging.

The workflow begins with the initial full-field-of-view (FFOV) imaging on a MCT machine at the best possible resolution achievable while covering the whole sample. This 3D MCT image provides an overview of sample heterogeneity, bedding layers and macroscopic differences in mineral concentration, and can usually be acquired in a few hours. The 3D data can be examined by virtually slicing in multiple orthogonal directions to decide the region of interest for sample extraction and check for big voids or cracks that can hinder subsequent sample preparation steps. In this example, we start from a 25 mm diameter and 5 mm high standard disk ([Figure 3](#)).

[Figure 3](#) shows the initial starting volume, the full-sample MCT scan and the rock features that can be observed at this resolution. Based on this 3D MCT image an ROI for subsampling is determined. Other available data, such as BSE mosaics, rock and thin-section descriptions may support the subsample selection.

### Step II - Mechanical drilling of sub volume.

Based on the examination of the full sample MCT images (and other available data sources), a 4 mm diameter sized cylindrical sub sample was extracted from the core plug by mechanical drilling. If the sample is homogeneous on the cm-to-mm scale, a subsample can be drilled randomly from the core plug. In this case, the workflow can start at this stage (Step II) without the MCT overview scan (Step I). However, detailed knowledge of the rock, a priori, is required to decide between random or prescriptive drilling. The extracted 4 mm sub cylinder was glued to an aluminum tube ([Figure 4](#)) and mounted in the MCT machine.

### Step III – Placement of fiducials and MCT imaging of 4 mm sub cylinder.

Before the 4 mm cylinder is imaged, distinct fiducial markers are placed on the sample surface. The fiducial markers enable to accurately locate the positions of the ROI. A general-purpose aluminum tape (50  $\mu\text{m}$  thickness) can be used as fiducial markers. Small pieces (~2 mm side length) of the aluminum tape with sharp perpendicular edges were fixed to the top surface, such that they could be used as visible fiducials for all subsequent sample preparation steps ([Figure 5](#)).

Accurate placement of the fiducials is essential since the edges are used as reference lines to position the sample along the laser motion axes during the next sub-sampling step. The sample marked with the fiducial was then imaged with the MCT at 2.5  $\mu\text{m}$  voxel resolution. This imaging step provides the 3D images to determine the location from where the next, smaller sub cylinder is extracted for subsequent higher-resolution imaging. After scanning, the sample assembly (including dimensions and exact position) is transferred to the laser micromachining device.

[Figure 6](#) shows the result of the 4 mm diameter MCT scan. After inspection of the volume, the ROI for further subsampling was selected using a common 3D-viewer software. The target ROI was chosen at a location 500  $\mu\text{m}$ ~2000  $\mu\text{m}$  below the top surface (shown by the yellow box in [Figure 6](#)).

The selected ROI as shown in the inset image consists of a large clay filled void and occupies an area of approximately 125  $\mu\text{m}$  x 250  $\mu\text{m}$ . The projected location of this ROI on the top surface is shown by the green and red crosshairs in the XY plane (upper left in [Figure 6](#)). The corner of aluminum tape seen in the XY slice was used as the reference point. Orthogonal distances with respect to the corner were measured in a 3D-viewer software. As a convention, we define the red cross-hair line as the X-axis and the green one as the Y-axis of the laser system. The next finer subsample to be extracted will be referred to as the “coarse pillar”.

#### Step IV – Locating the ROI in the laser system and coarse pillar extraction process.

The 4 mm sample was transferred to the laser micro-machining system while still mounted on the pin vice. This ensures that no sample misalignments occur and the same coordinate system is maintained between the MCT and laser system. The pin vice was placed on the X-Y stage of the laser system as shown in [Figure 7](#). Using the visual light microscope (VLM) in the laser system, the pin vice was centered under the crosshair and rotated to align the edges of the aluminum tape to match the red cross-hair of the laser system.

After the position was determined, the base was fixed by tape to avoid sample motion during stage movement. Once the fiducial aluminum corner was centered and aligned, the laser stage X and Y positions were moved in the horizontal and vertical directions by entering the offsets measured in the previous step ([Figure 7B](#)). Applying the standard sample preparation method at low power, a 0.8 mm coarse pillar was milled top-down inside a 2.4 mm diameter trench with the laser beam steered by a galvo steering lens. [Figure 7C](#) shows the top-down milled coarse pillar (still in its original place inside the trench), which was then glued to a 0.7 mm steel pin using an automated procedure ([Figure 7D](#)).

Due to the characteristic divergence of the focused laser beam beyond its focal plane, certain limitations exist regarding the total height of a pillar that can be milled out using this technique (around 3 mm for the system described here). It is therefore recommended to locate the ROI in the previous MCT scanning step such that it is within the range of 0.5 – 2 mm below the top surface of the sample. For samples where the volume to be extracted lies much below the 3 mm limit, the surface may need to be ground down to sufficient depth before proceeding with laser milling. [Figure 8](#) schematically shows the setup of top-down milling in the laser micromachining device.

#### Step V – MCT imaging of coarse pillar to confirm the location of the selected ROI.

The 0.8 mm milled coarse pillar, glued to the 0.7 mm steel pin was then removed from its original position inside the 4 mm sample with fine-tipped tweezers. The extracted 0.8 mm coarse pillar and the original 4 mm sample are shown in [Figure 9A](#). The 0.8 mm coarse pillar ([Figure 9B](#)) is then placed into the MCT and imaged at a voxel size of 3  $\mu\text{m}$  in FFOV mode. [Figure 9C](#) shows the results of the coarse pillar MCT scan. This quick scan is necessary to check if the selected ROI corresponds to the center of rotation axis of the pin ([Figure 9C](#)) and to measure the extent of misalignment. Some degree of misalignment ( $<50 \mu\text{m}$ ) between the axis of the pin and the coarse pillar is expected due to the gluing operation. If the misalignment is more than approximately 50  $\mu\text{m}$ , a different region of interest along the vertical axis of rotation of the pin may be chosen or the coarse pillar has to be remounted, after which the MCT control scan is repeated to locate the ROI in the re-glued pillar.

[Figure 10](#) illustrates why the ROI needs to be in the center of rotation axis of the pin. The lathe-style operation to extract the fine pillar offers only a single degree of freedom, i.e. along the axis of rotation of the coarse pillar (indicated by the transparent blue zone in [Figure 10](#)). Any region lying out of the rotational axis cannot be machined into a fine pillar, for example, as indicated by the red cylindrical volume in [Figure 10](#). Under such a circumstance, it would be required to remount the coarse pillar on the pin with sufficient offset, so that the axis of the desired volume of interest coincides with the center of rotation of the pin.

#### Step VI – Trim coarse pillar length and run fine pillar process.

Following imaging the coarse pillar was milled down in diameter using a lathe-style approach to fit the nanoCT field of view dimensions of <65 $\mu$ m. The coarse pillar was mounted on the laser lathe by inserting the glued pin into the chuck. Before the fine pillar milling process, the material above the ROI needs to be trimmed. The fractured end was located under the crosshair and trimmed, exposing the top of the desired region of interest ([Figure 11A, B](#)). A fine pillar with a 65  $\mu$ m diameter was then produced, using low power lathe-style milling ([Figure 11C](#)). The resulting fine pillar is readily compatible with the standard nanoCT pin vice and is ready for the final nanoCT imaging.

#### Step VII – nanoCT imaging of fine pillar.

The fine pillar was gently removed from the lathe chuck of the laser machine and mounted in the nanoCT pin vice holder. Using mosaic mode the desired region of interest was chosen for a single large field of view scan at a voxel size of 65nm. [Figure 12](#) presents the nanoCT imaging results of the fine pillar. The orthogonal slices and the volume rendering show the targeted kaolinite clay structures, which provide the gateways for flow in this tight sand sample.

### **Discussion and Conclusions**

Precisely controlled sub-sampling is mandatory for construction of representative multiscale digital rock models from images, a pre-requisite for calculation of meaningful petrophysical properties and fluid flow in DRP and pore network modeling. Based on the specific heterogeneity and other characteristics of the reservoir samples, the workflow can be tailored to image at different sample size and resolution levels.

### **References Cited**

- Al-Ratrou, A.A., M.Z. Kalam, J.S. Gomes, M.S. Jouini, and S. Roth, 2014, Narrowing the Loop for Microporosity Quantification in Carbonate Reservoirs Using Digital Rock Physics and Other Conventional Techniques – Part II: International Petroleum Technology Conference, Doha, Qatar, IPTC 17702, 11 p.
- Blunt, M. J., B. Bijeljic, H. Dong, O. Gharbi, S. Iglauer, P. Mostaghimi, A. Paluszny, and C. Pentland, 2013, Pore-scale imaging and modelling: *Advances in Water Resources*, v. 51, p. 197-216.
- Kalam, M.Z., T. Al Dayyani, A. Clark, S. Roth, C. Nardi, O. Lopez, and P.E. Øren, 2010, Case study in validating capillary pressure, relative permeability and resistivity index of carbonates from X-Ray micro-tomography images: SCA2010-02 presented at the 2010 SCA International Symposium of the Society of Core Analysts, Halifax, Canada.
- Kalam, M.Z., 2012, Digital Rock Physics for Fast and Accurate Special Core Analysis in Carbonates: New Technologies in the Oil and Gas Industry, Dr. Jorge Salgado Gomes (Ed.), InTech, DOI: 10.5772/52949.

Schembre-McCabe, J., R. Salazar-Tio, and J. Kamath, 2012, Two examples of adding value through digital rock technology: SCA2012-18 presented at the 2012 International Symposium of the Society of Core Analysts, Aberdeen, Scotland, UK.



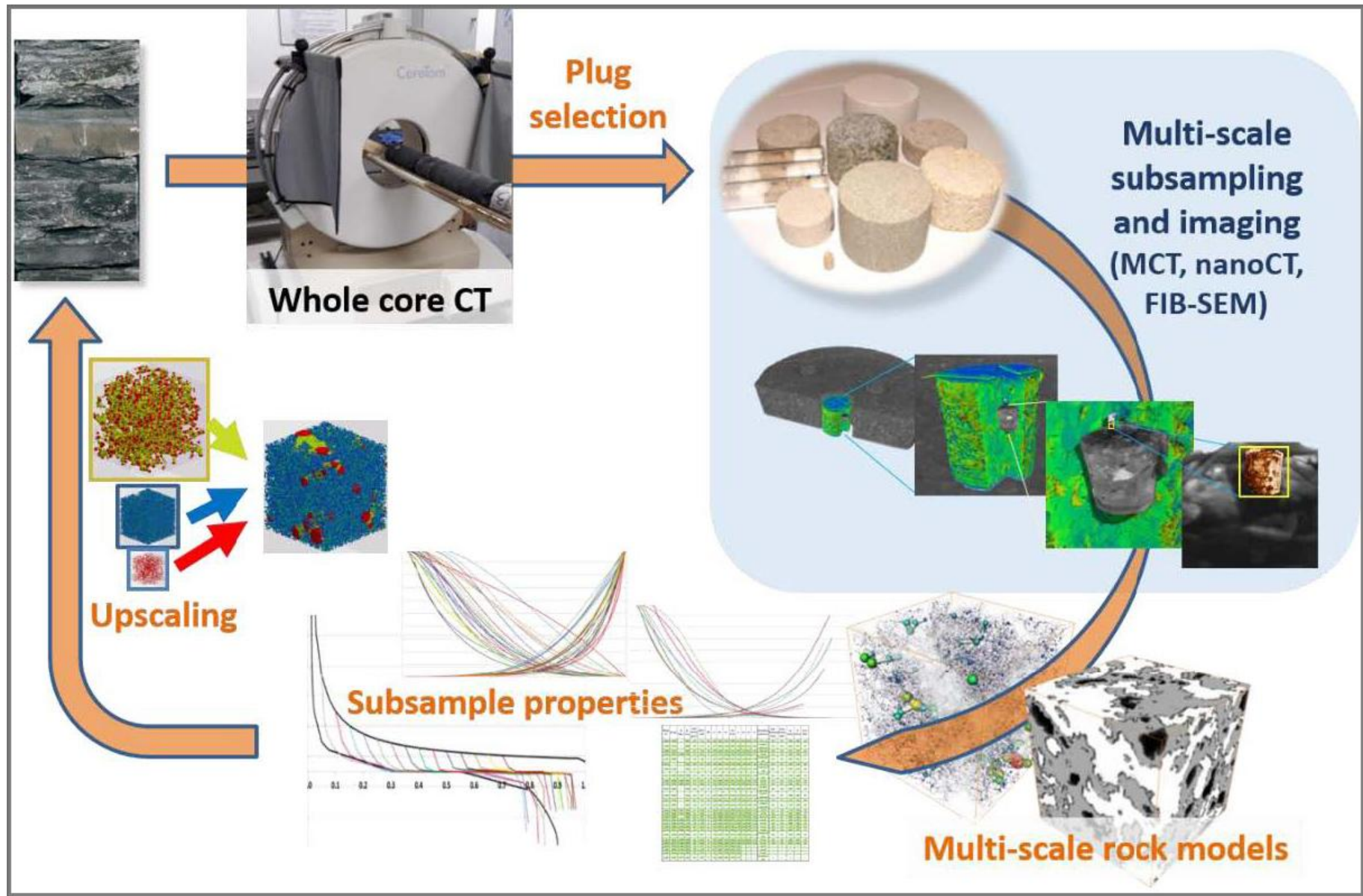


Figure 1. Position of multi-scale subsampling and imaging module (blue shaded area) in a generalized DRP work flow chart.



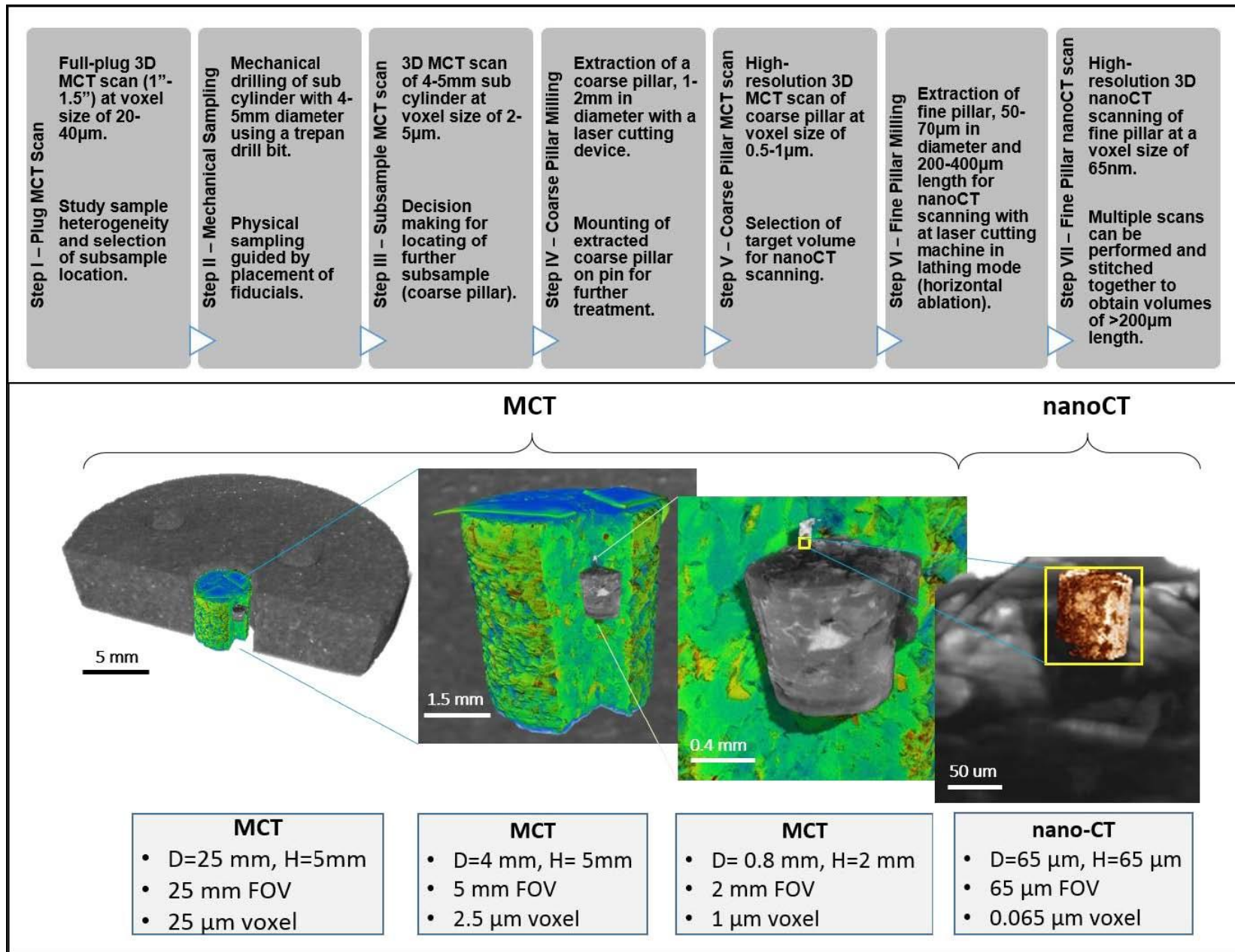


Figure 2. Schematic workflow (top panel) and graphical representation of entire sampling and imaging procedure from full-plug sample to smallest volume and nanoCT scan.

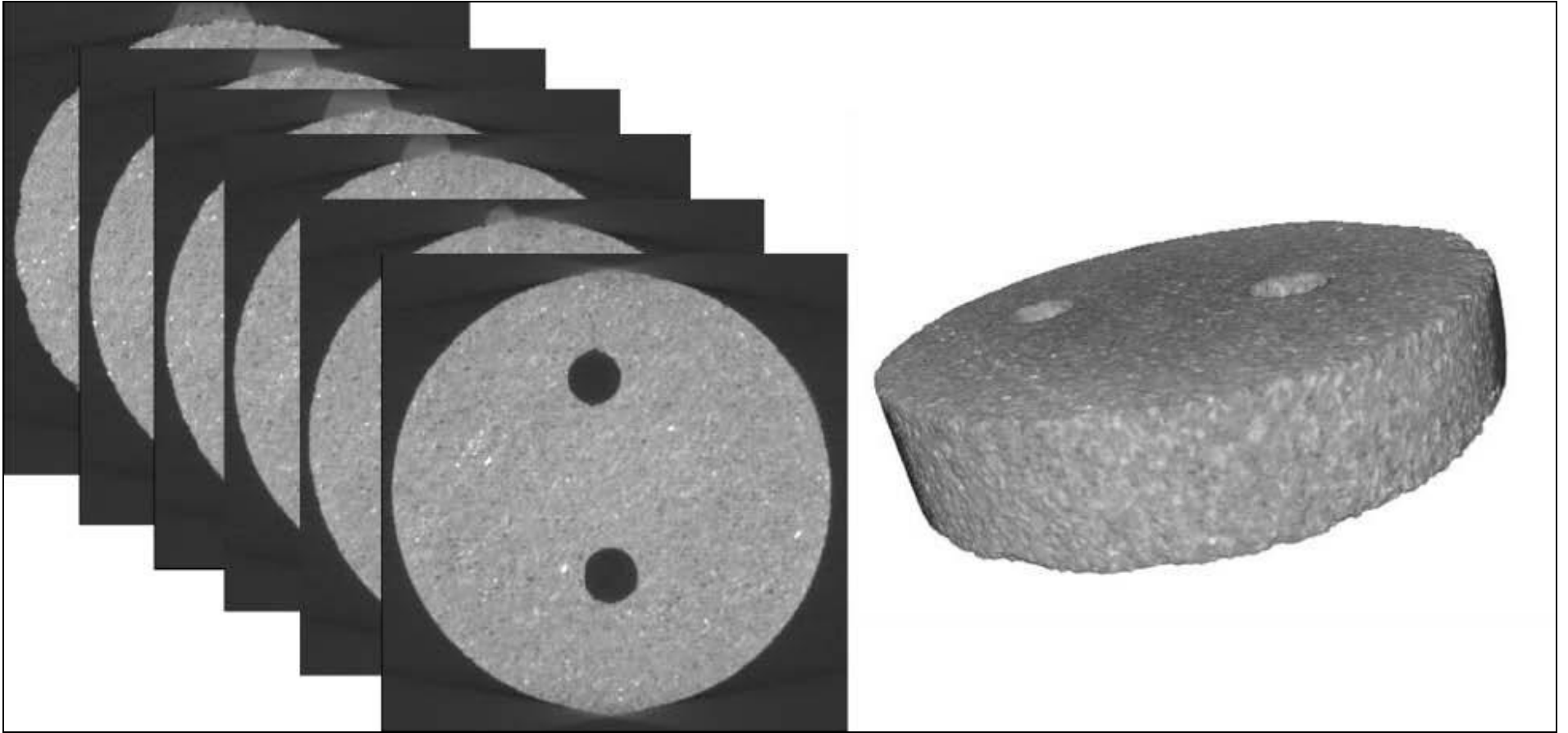


Figure 3. Full sample MCT overview scan of 25 mm diameter and 5 mm high disk. Voxel size is 25  $\mu\text{m}$ .

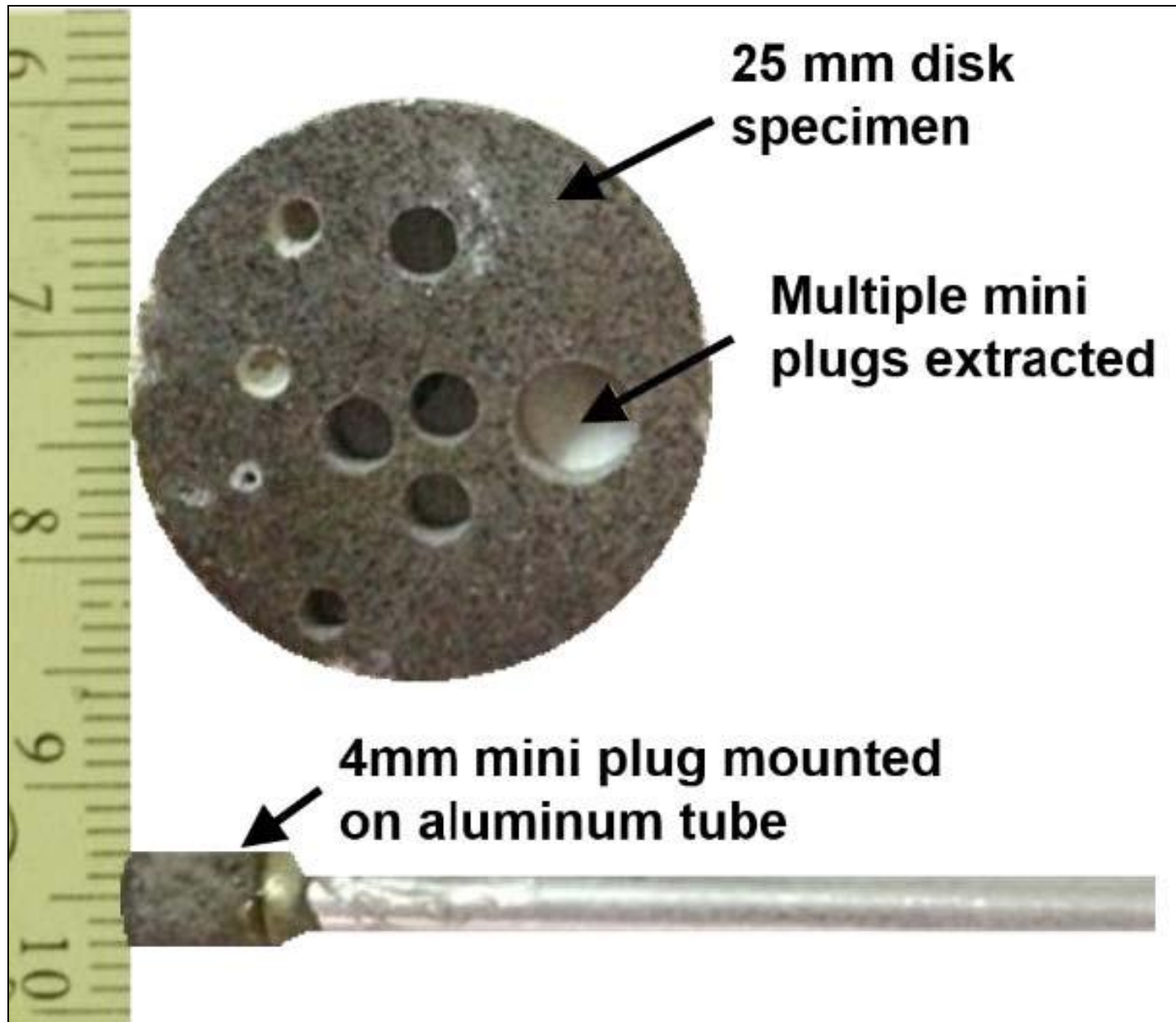


Figure 4. Starting 25 mm diameter x 5 mm specimen (upper) and 4 mm drilled sub cylinder mounted onto a pin vice for FFOV MCT scan (lower).

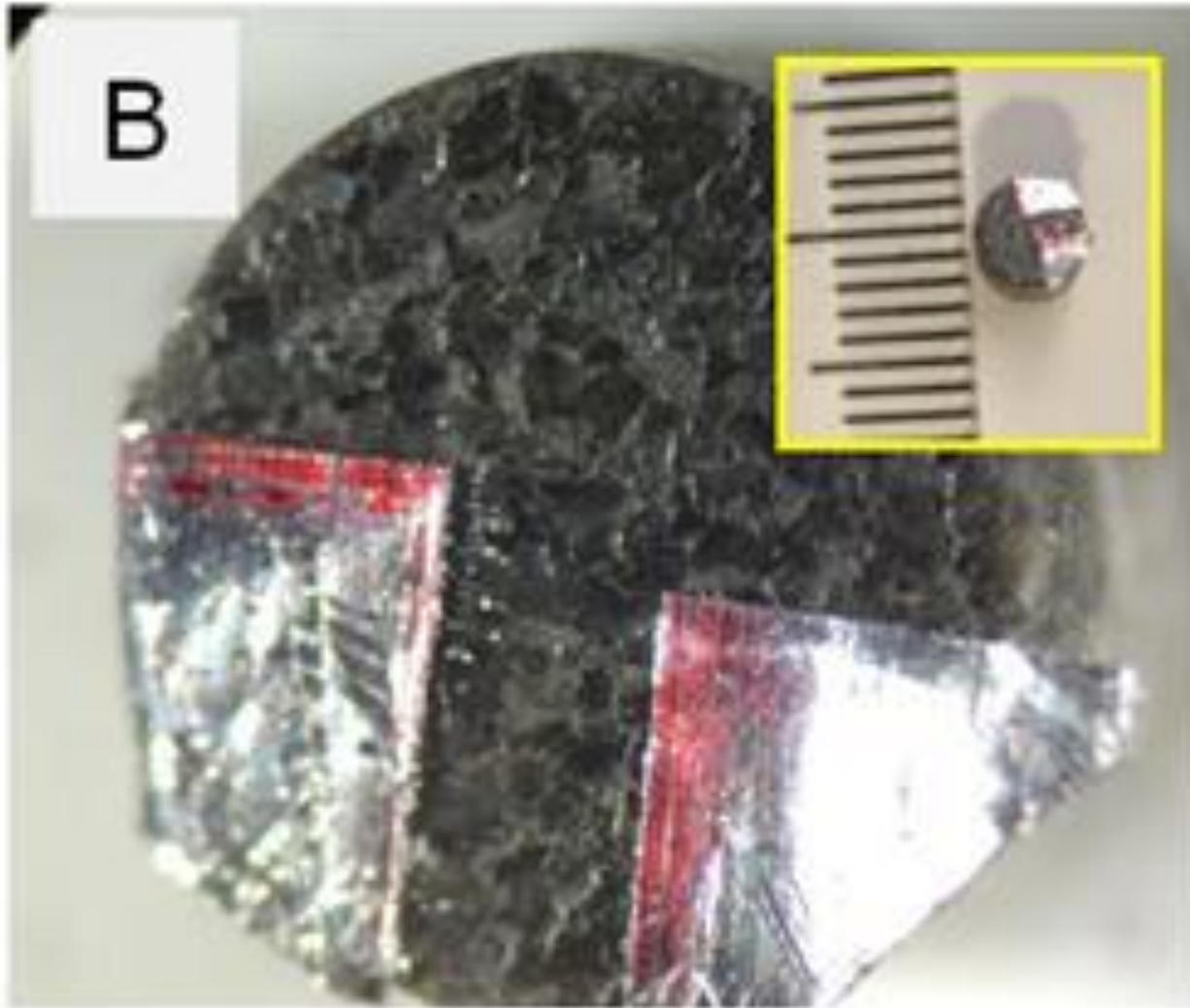


Figure 5. Placement of fiducials on top side of the 4 mm sub cylinder.



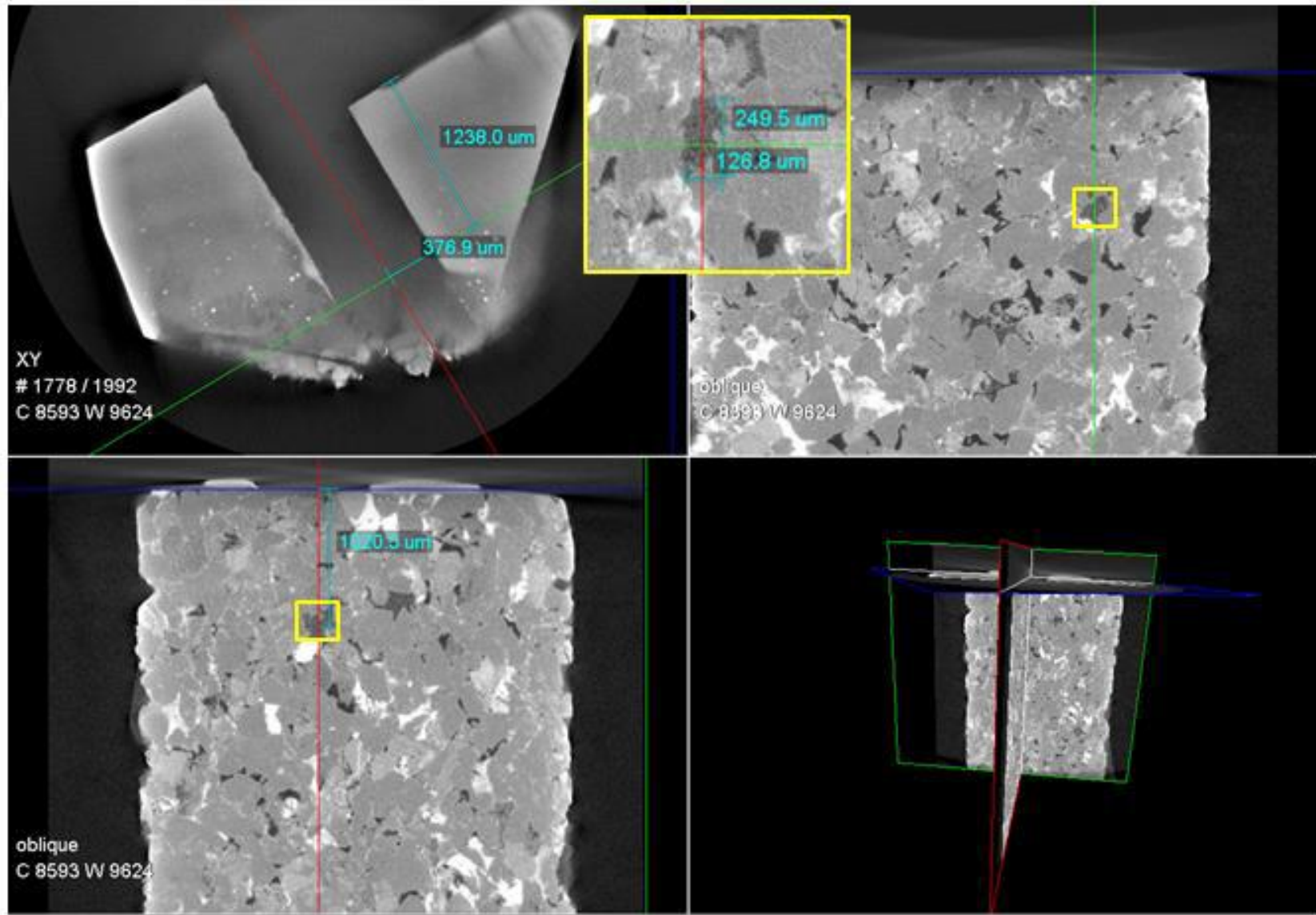


Figure 6. Fiducial position in MCT scan (upper left) and cross sectional views of the MCT imaging results of 4 mm sub cylinder imaged at 2.5  $\mu\text{m}$  voxel size (upper right and lower panel). The yellow box depicts the ROI (clay-filled pore) selected for further subsampling.

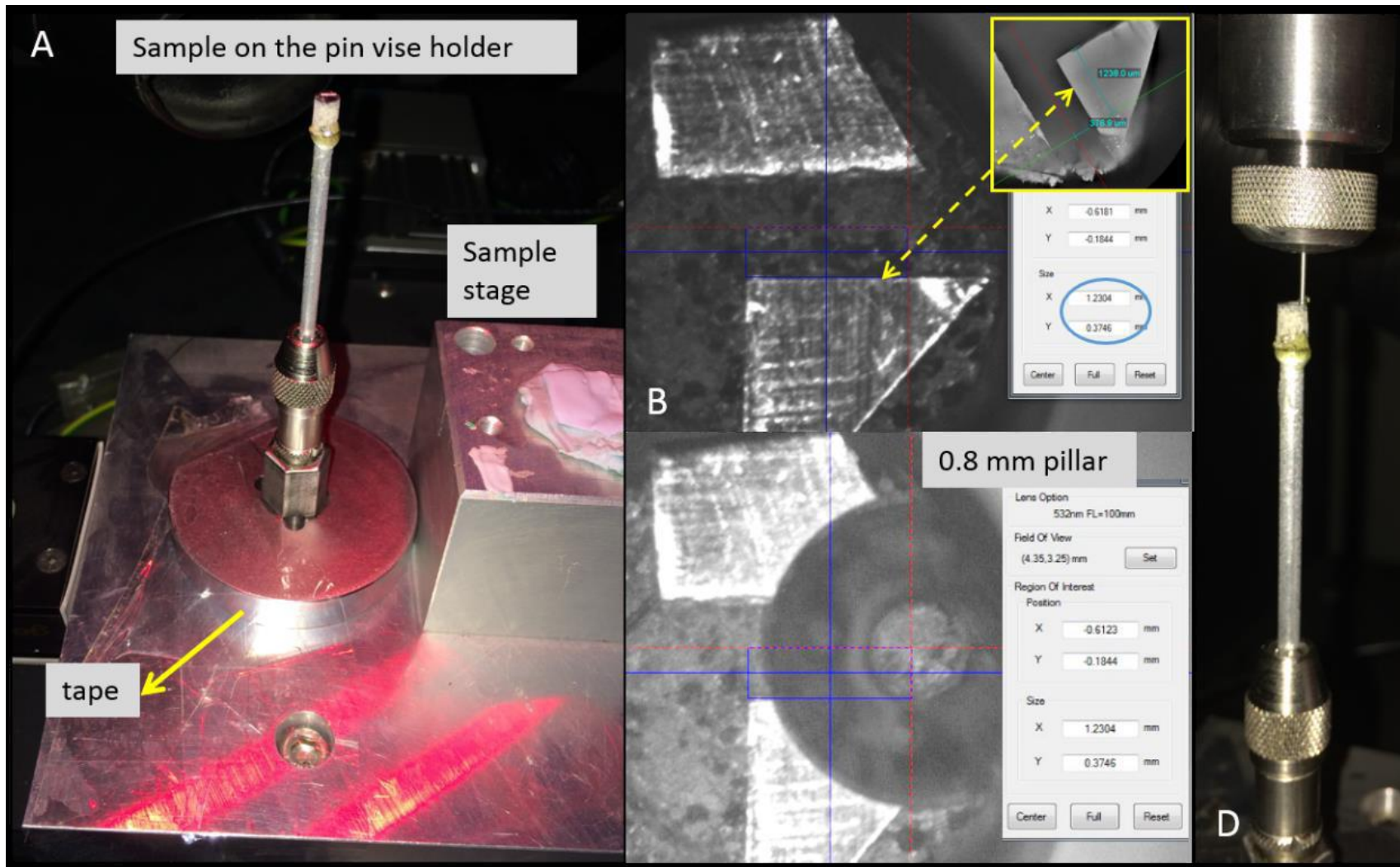


Figure 7. Locating the coarse pillar ROI and setup of the extraction process. (A) sample mounted on the pin vise MCT sample holder beside the laser sample stage, the base fixed with a piece of tape; (B) and (C) locating the ROI and run coarse pillar extraction process; (D) coarse pillar glued to the 0.7 mm pin.



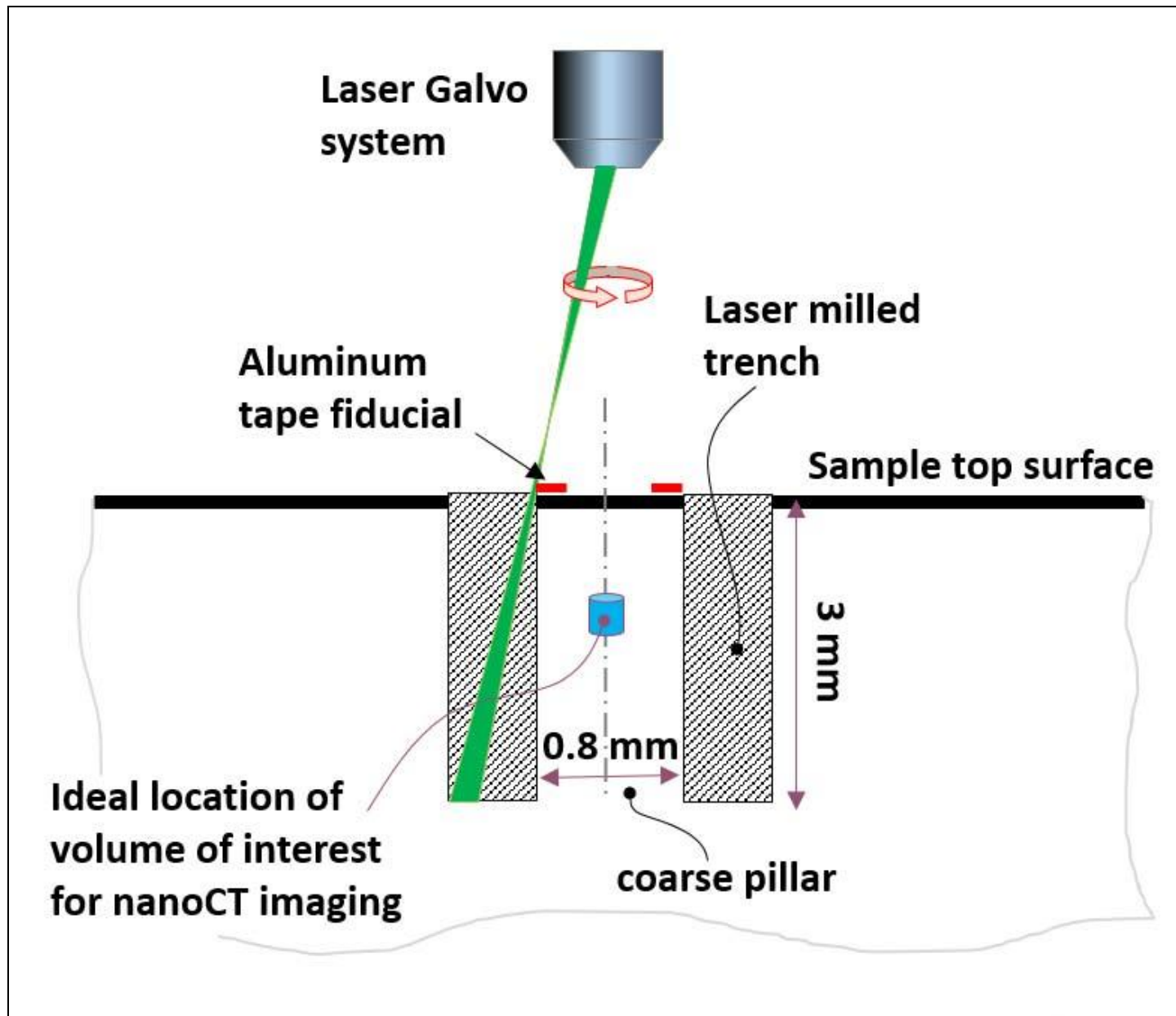


Figure 8. Schematic illustration of top-down milling in the laser machine. The blue sample is the ultimate target for nanoCT scanning at the end of the workflow and is ideally located within 3 mm below the sample surface.

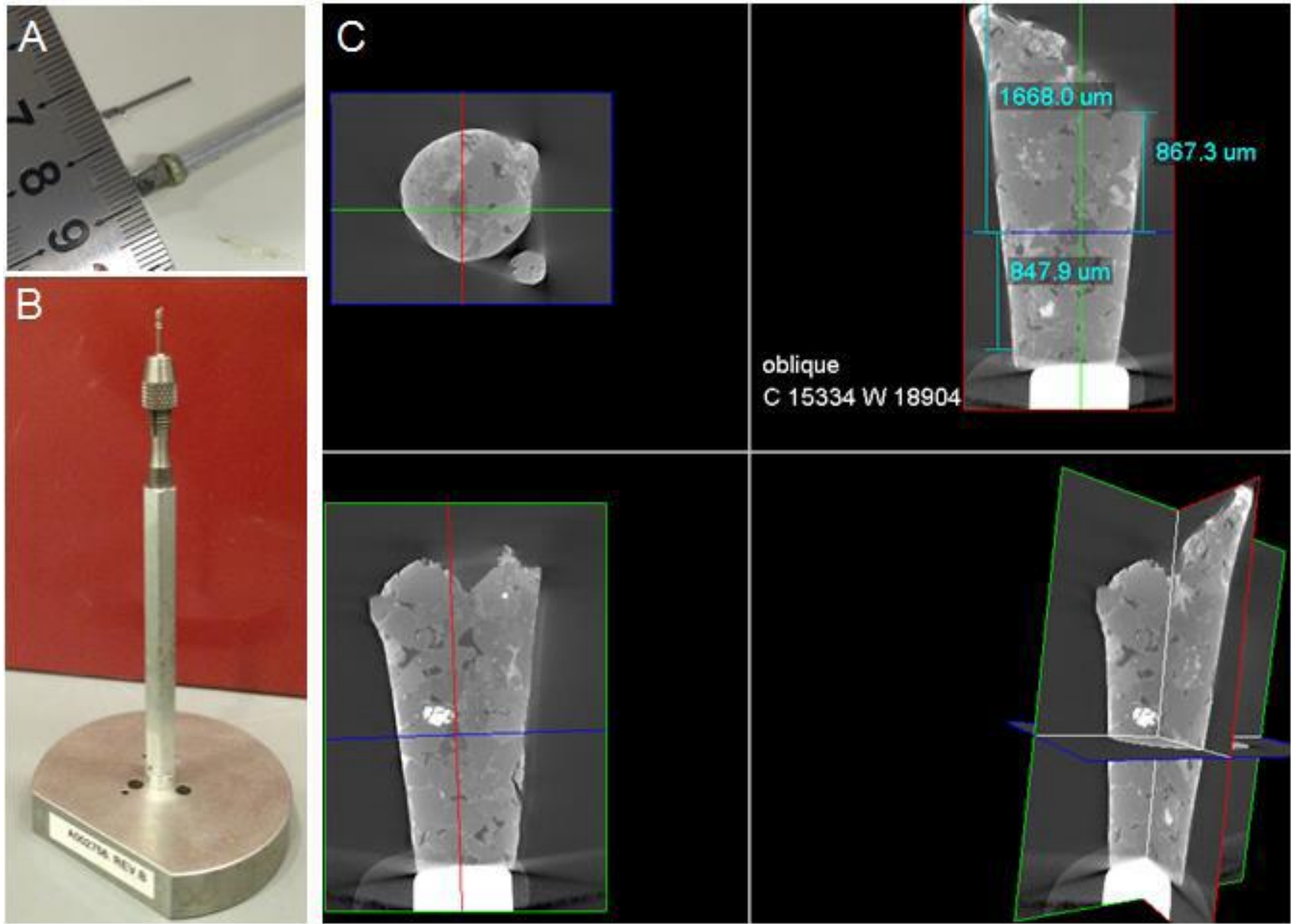


Figure 9. (A) Comparison of 4 mm subsample on the Al tube and coarse pillar glued on the 0.7 mm pin; (B) coarse pillar in the MCT mini pin vise holder; (C) MCT results of coarse pillar scan in 3D viewer to locate ROI position.

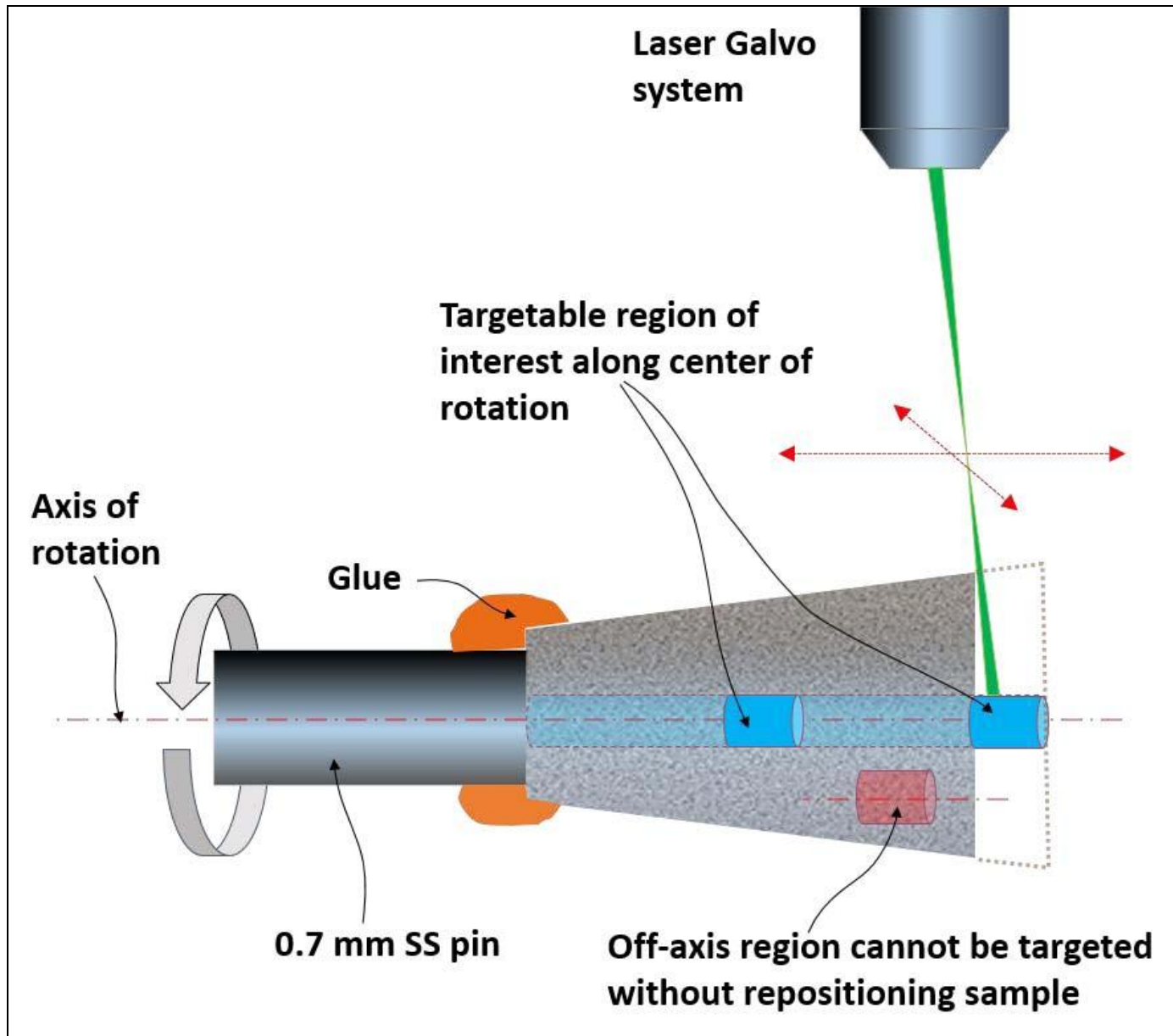


Figure 10. Schematic illustration of the laser-milling process in the lathe-style mode. The sample is turned around the axis of rotation while the laser beam is abrading the material from outside to inside. The final targets in the resulting fine pillar are shown in blue. Red area depicts an off-axis region that cannot be extracted with this technique.

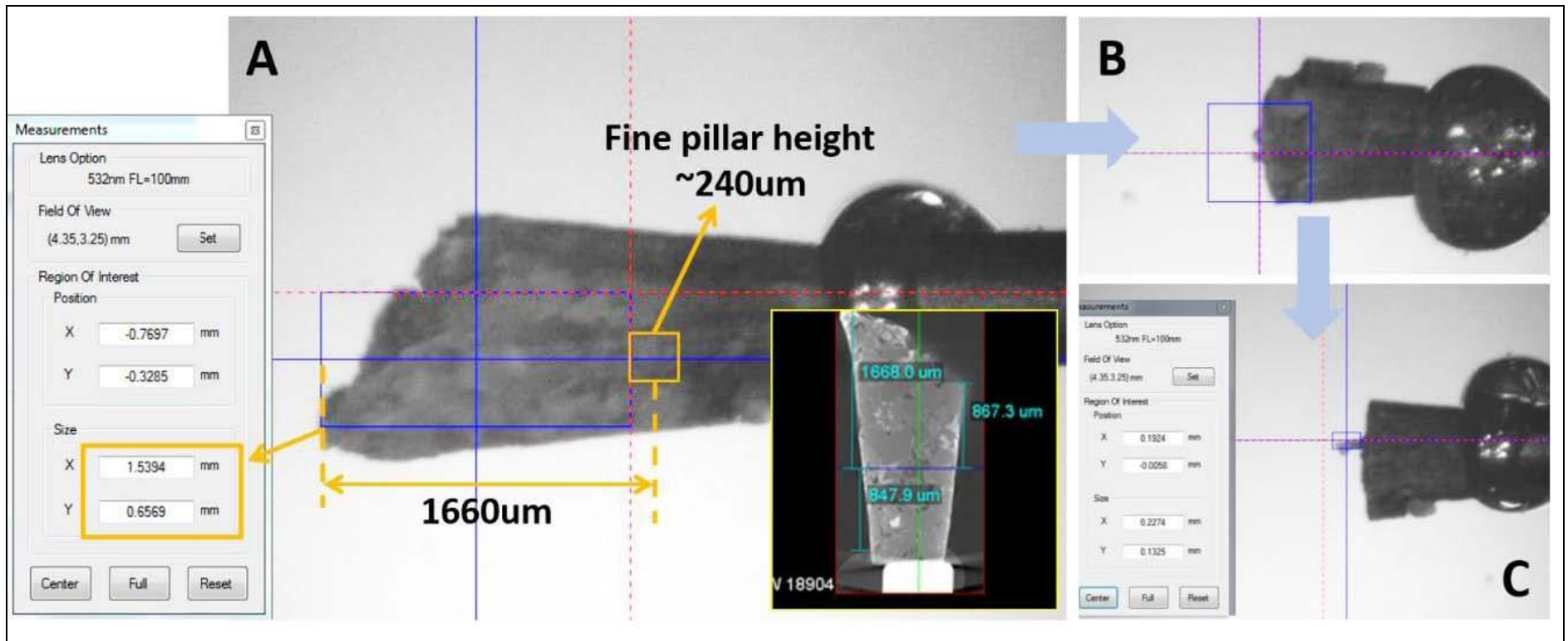


Figure 11. Trimming of the tip and fine pillar process to produce the 65  $\mu\text{m}$  pillar for nanoCT imaging. (A) Locate the ROI by the tip as a fiducial; (B) trimmed sample; (C) sample after fine pillar milling process.

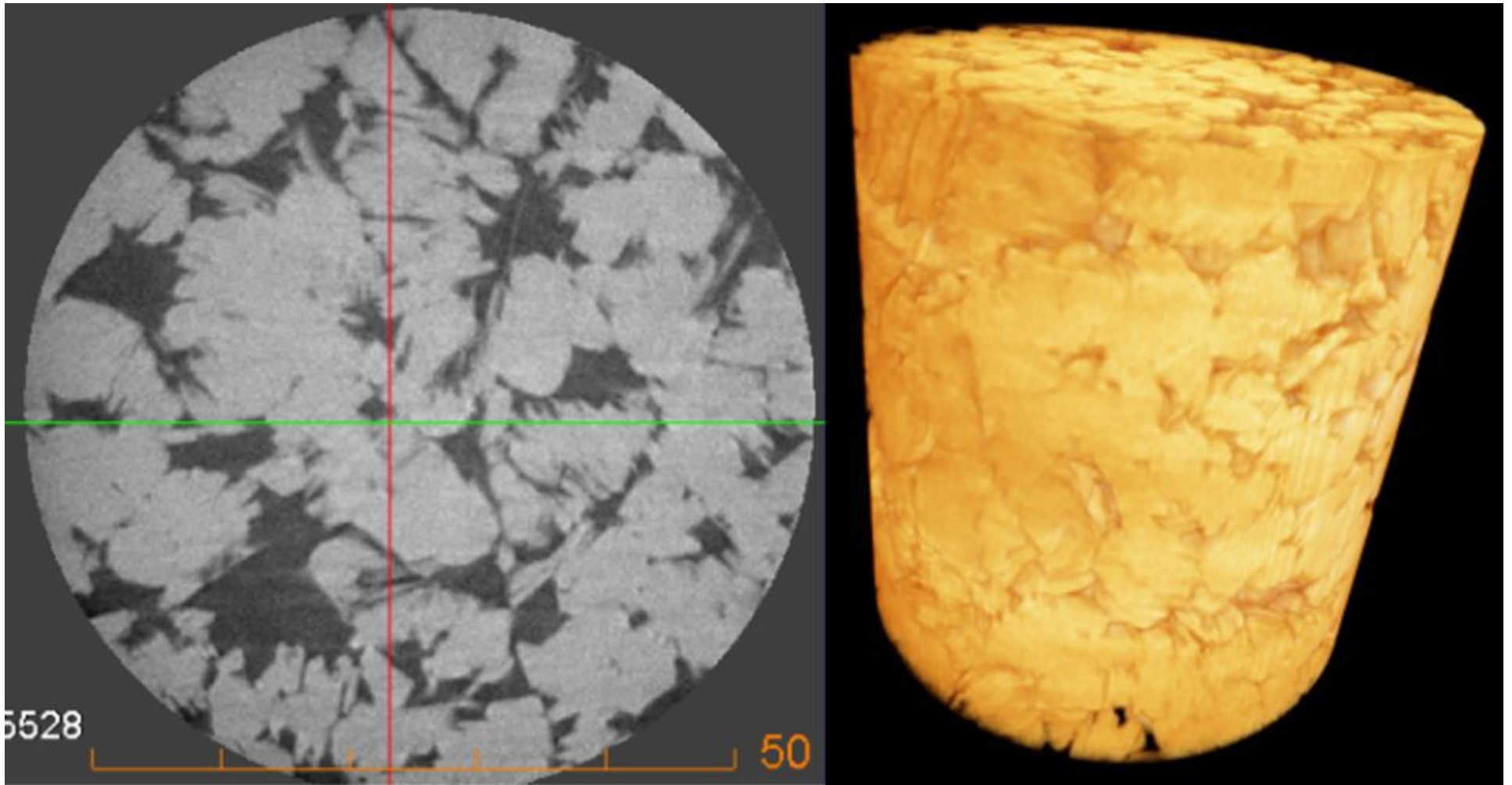


Figure 12. Results of 3D nanoCT scan of fine pillar target volume: cross sectional image of kaolinite clay structure (left) and 3D rendered volume (lower right). Scale bar is 50 $\mu$ m.